

Universality of flux-fluctuation law in complex dynamical systems

Zhao Zhou,¹ Zi-Gang Huang,^{1,*} Liang Huang,^{1,2} Ying-Cheng Lai,^{2,3} Lei Yang,⁴ and De-Sheng Xue^{1,†}

¹*School of Physical Science and Technology, Lanzhou University, Lanzhou 730000, China*

²*School of Electrical, Computer and Energy Engineering, Arizona State University, Tempe, Arizona 85287, USA*

³*Department of Physics, Arizona State University, Tempe, Arizona 85287, USA*

⁴*Institute of Modern Physics, Chinese Academy of Sciences, Lanzhou 730000, China*

(Received 22 August 2012; revised manuscript received 13 November 2012; published 17 January 2013)

Recent work has revealed a law governing flux fluctuation and the average flux in complex dynamical systems. We establish the universality of this flux-fluctuation law through the following steps: (i) We derive the law in a more general setting, showing that it depends on a single parameter characterizing the external driving; (ii) we conduct extensive numerical computations using distinct external driving, different network topologies, and multiple traffic routing strategies; and (iii) we analyze data from an actual vehicle traffic system in a major city in China to lend more credence to the universality of the flux-fluctuation law. Additional factors considered include flux fluctuation on links, window size effect, and hidden topological structures such as nodal degree correlation. Besides its fundamental importance in complex systems, the flux-fluctuation law can be used to infer certain intrinsic property of the system for potential applications such as control of complex systems for improved performance.

DOI: [10.1103/PhysRevE.87.012808](https://doi.org/10.1103/PhysRevE.87.012808)

PACS number(s): 89.75.Hc, 89.20.Hh, 89.75.Da

I. INTRODUCTION

In a finite physical system observed and probed in finite time, fluctuations in quantities of interest are ubiquitous. For a complete random process such as one that follows the standard Gaussian distribution, its average and variance are parameters that are independent of each other. In this case, the fluctuations are an intrinsic property of the random process, which does not depend on its average. However, when the process contains a deterministic component, such as those occurring on complex dynamical systems, the mean and variance of a physical variable are typically correlated. Consider, for example, traffic flow on a complex network. As the average flux is increased, the fluctuations tend to intensify as well. Exploration of issues such as the characterization of fluctuations in complex dynamical systems, the precise relation between the average and variance, and the effect of fluctuations on system dynamics, has formed a particular area of recent research [1–8].

An issue of significant physical interest is whether there exists a universal scaling law between the fluctuation and the average flux [1–6]. In particular, the importance of fluctuations in complex dynamical systems was recognized and a power-law scaling relation between the fluctuation and the average flux was reported [1], where the power-law exponent can take on a finite set of discrete values, such as 1/2 or 1 [1]. Subsequently, it was shown [2] that, in contrast to the result in Ref. [1], the power-law exponent can assume continuous values in the range [1/2, 1] [2]. Quite recently, the notion of power-law scaling between the fluctuation and the average flux was refuted and a non-power-law type of relation between the two quantities was obtained by Meloni *et al.* [3]. Besides providing an analytical argument, the authors also presented numerical support from both model systems and a realistic communication network system for the flux-fluctuation law [3].

In this paper, we generalize the flux-fluctuation law, first obtained in Ref. [3], and address the universality of this law as applied to general complex networked systems. Our approach consists of three steps. (i) We present a straightforward but more general derivation of the relation, which does not rely on system details. In particular, let f_i denote the flux of some kind of physical flow of node i in a complex network and let $\langle f_i \rangle$ and σ_i be the average flux and the corresponding fluctuation, respectively. The law between $\langle f_i \rangle$ and σ_i is then given by

$$\sigma_i = \sqrt{\langle f_i \rangle + \alpha^2 \langle f_i \rangle^2}, \quad (1)$$

where $\alpha \equiv (\sigma_{R_T})/\langle R_T \rangle$ is a single parameter determined by the property of the external driving $R(t)$ only, and σ_{R_T} and $\langle R_T \rangle$ are the standard deviation and the expectation value of $R(t)$, respectively. We note that, in Ref. [3], the flux-fluctuation law has the same form as Eq. (1), but it was derived based on a random-diffusion picture under the assumption of uniformly distributed external driving. In our expression, the parameter is generally given by the ratio between the variance and the mean square of the external driving. Equation (1) is thus more general. (ii) We carry out extensive numerical computation using various network models and traffic dynamics to establish the validity of Eq. (1). (iii) We demonstrate that the flux-fluctuation law holds for real traffic flow in a major city in China and we point out the special caveats that must be taken into account in order to observe Eq. (1) in real physical systems. Our results corroborate those in Ref. [3] in that the relation between flux fluctuation and average in general is not a power law, but these two basic quantities obey a law that is apparently universal in complex physical systems.

II. THEORY

We begin by demonstrating how Eq. (1) can be obtained in a more general setting than that of Ref. [3]. Here we assume that the traffic dynamics of the system is conservative and packets can flow from one node to another if there is a connection between them.

*huangzg@lzu.edu.cn

†xueds@lzu.edu.cn

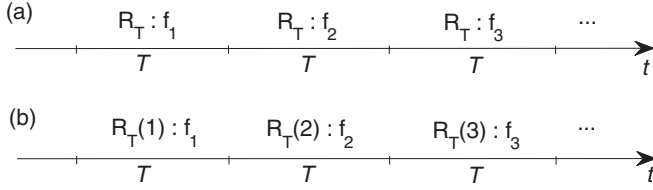


FIG. 1. Schematic illustration of obtaining flux f observationally with respect to external driving R_T : (a) R_T is constant and f is random variable with Poisson distribution and (b) R_T is assumed to change with time.

We first consider the simple case of a single-node traffic-flow model in the free-flow state without any congestion. Let $R(t)$ be the probability that, during a time unit, a package passes through this node. Let T be the length of the time window of measurement of flux f_i and σ_i be the deviation of f_i from its average. For an arbitrary time window $[t, t + T]$, there are on average $R_T = \int_t^{t+T} R(\tau) d\tau$ packets passing through this node. The quantity R_T can thus be regarded as a kind of *external driving* that represents systematic or random variations upon the system from the outside environment, which determines the total flux of the system in a given period. For example, in a river network, the external driving can be the precipitation in the basin region, while for traffic flow in a city, the external driving can be the daily rhythmic behavior of human activities such as commuting between one's place of residence and place of work. External driving should be distinguished from intrinsic fluctuations of the system. For traffic flow on the network, such intrinsic fluctuations are caused, for example, by randomness in the package-generating process and in the selection of paths.

The external driving R_T does not need to be uniform in time. Let $P_{R_T}(r)$ be the probability of $R_T = r$. If R_T is constant, f_i follows the standard Poisson process so that the expectation of f_i is $\langle f \rangle = R_T$, as shown in Fig. 1(a). The probability of $f_i = n$ is then given by the Poisson distribution $P_\pi(n, R_T) = e^{-R_T} R_T^n / n!$. In the more general case where R_T is time dependent, as shown in Fig. 1(b), we can regard it as a random variable with some kind of probability distribution $P_{R_T}(r)$, which can be quite arbitrary. In this case, the probability of $f_n = n$ can be expressed as

$$P_{f_i}(n) = \int_0^\infty P_\pi(n, r) P_{R_T}(r) dr, \quad (2)$$

which allows us to calculate the average and variance of f_i in a straightforward manner. In particular, we have

$$\begin{aligned} \langle f_i \rangle &= \sum_{n=0}^{\infty} n P_{f_i}(n) \\ &= \sum_{n=0}^{\infty} n \int_0^\infty P_\pi(n, r) P_{R_T}(r) dr \\ &= \int_0^\infty \left(\sum_{n=0}^{\infty} n P_\pi(n, r) \right) P_{R_T}(r) dr \\ &= \int_0^\infty r P_{R_T}(r) dr = \langle R_T \rangle \end{aligned} \quad (3)$$

and

$$\begin{aligned} \langle f_i^2 \rangle &= \sum_{n=0}^{\infty} n^2 P_{f_i}(n) \\ &= \sum_{n=0}^{\infty} n^2 \int_0^\infty P_\pi(n, r) P_{R_T}(r) dr \\ &= \int_0^\infty \left(\sum_{n=0}^{\infty} n^2 P_\pi(n, r) \right) P_{R_T}(r) dr \\ &= \int_0^\infty (r + r^2) P_{R_T}(r) dr \\ &= \langle R_T \rangle + \langle R_T^2 \rangle. \end{aligned} \quad (4)$$

We thus have

$$\sigma_i^2 \equiv \langle f_i^2 \rangle - \langle f_i \rangle^2 = \langle f_i \rangle + \langle f_i \rangle^2 \frac{\sigma_{R_T}^2}{\langle R_T \rangle^2}, \quad (5)$$

which is Eq. (1).

The above argument suggests that, in the case of an arbitrary packet-generation distribution, there is a single parameter in the relationship between σ_i and $\langle f_i \rangle$, which is the ratio between the standard deviation and the mean of R_T . Depending on this ratio, the asymptotic expression of Eq. (1) has two scaling forms. In particular, for small α or f_i , Eq. (1) becomes

$$\sigma_i = \sqrt{\langle f_i \rangle},$$

a power-law scaling with the exponent 1/2. For large α or f_i , Eq. (1) reduces to

$$\sigma_i = \alpha \langle f_i \rangle.$$

The previously observed [1,2] two forms of the power-law scaling between the flux fluctuation and the average flux are thus two limiting cases of Eq. (1) in terms of the ratio α .

Equation (1) is for a single node under external driving. In a complex networked system, packets flow among various nodes, e.g., data packets in the Internet, traffic flow in a city, and stream flows in a branched river. If the system is under a *single* and spatially *uniform* external driving, the effective driving on different nodes will be different, e.g., nodes with a larger basin will have a larger flux. However, we expect the statistical properties of the driving forces at the level of individual node to be the same. That is, the ratio α should be node independent, which can be argued as follows. For a given total number of packets N_p , when the routing protocol is fixed, the average number of packets $\langle f_i \rangle$ on a node i is given and because of the randomness in the selection of the source and destination of the packets, f_i is a random variable following a Poisson distribution. The parameter R_T characterizes N_p . The variation in R_T corresponds to the variation in the total number of packets in the network and hence it is a global parameter and is the same for all nodes, as is α ($=\sigma_{R_T}/\langle R_T \rangle$). This reasoning is independent of network topology and routing protocol and is thus valid for different variations in network topology and routing protocol. For example, if the network has correlation and hidden structures, the flux of two neighboring nodes f_i and f_j may be correlated, however, the dependence of σ_i on $\langle f_i \rangle$ and σ_j on $\langle f_j \rangle$ will both follow Eq. (1) with the same parameter α . Specifically, if we plot $(\langle f_i \rangle, \sigma_i)$ for every

node, all points should fall on the same curve with a single value of the ratio α .

Note that the above analysis is based on two observations: (i) For a given total number of packets N_p and a given routing protocol, the average flux $\langle f_i \rangle$ at node i is fixed and $\langle f_i \rangle \sim N_p$ and (ii) because of the randomness in selecting a source and destination for each packet, f_i is a random variable following a Poisson distribution. As indicated in Ref. [6], if we consider the flux behavior through links in network instead of nodes, the above two observations still hold, e.g., $\langle f_{ij} \rangle \sim N_p$ and f_{ij} is a random variable following a Poisson distribution. Therefore Eq. (1) should hold with respect to links with the same parameter α .

Our derivation of Eq. (1), while straightforward, provides a deeper understanding of the physical origin of the flux-fluctuation law. It can also be seen that the dynamical details of the external driving within the observational time window have no effect on the form of the law. Note, however, that the size of the window matters. Assume we have a given $R(t)$ for a different observational time window; the resulting external driving R_T will be different, leading to a different value of $\alpha = \sigma_{R_T} / \langle R_T \rangle$. Since Eq. (1) only depends on α , the resulting plot $(\sigma_i, \langle f_i \rangle)$ will be different, but the form of the equation will be the same. Another point is that for a larger window, the average flux $\langle f_i \rangle$ will be larger. When the change in α is small, the power-law fitting can yield exponent 0.5 for a small window and exponent 1 for large observational windows, as noted by Kujawski *et al.* [6]. In the special case treated in Ref. [3] where the external driving R_T is uniformly distributed in the range $[W - \delta, W + \delta]$, we have $(\sigma_{R_T})^2 = \delta^2/3$ and $\langle R_T \rangle = W$. Equation (1) then reduces to Eq. (7) in Ref. [3].

III. NUMERICAL TESTS OF UNIVERSALITY

To demonstrate the universality of Eq. (1), we carry out numerical simulations of packet-flow dynamics [9] on a number of standard complex network models, namely, scale-free, random, and small-world networks. In each case, at each time step, the system generates R packets whose

sources and destinations are selected randomly. The packets start to flow in the network until they reach their respective destinations. The delivery capacity of the nodes is assumed to be infinity and packets are delivered according to a certain routing strategy. In our simulation, we have considered two specific protocols: shortest-path and efficient protocols, where for the latter a path along which the sum of degrees is minimum [10] is selected. The computations are performed for different R_T distributions (uniform, Poisson, power-law) on networks of different topologies. In our simulation, we set $T = 100$ and $\langle R_T \rangle = 10T$. For a uniform distribution, the range of R_T is $\langle R_T \rangle [1 - \sqrt{0.3}, 1 + \sqrt{0.3}]$. For a Poisson distribution, $R_T = \langle R_T \rangle x$, where x follows the Poisson distribution with $\langle x \rangle = 10$. In the case of a power-law distribution, $R_T = \langle R_T \rangle \times x(\gamma - 2)/(\gamma - 1)$, where x follows the distribution function $(\gamma - 1)x^{-\gamma}$ and $\gamma = 5.3166$. The above parameters give rise to $\alpha^2 = (\sigma_{R_T})^2 / \langle R_T \rangle^2 = 0.1$ for all three cases so that a meaningful comparison can be made. In addition, in order to show that the details of the flow dynamics in the observational time window have no effect on Eq. (1), we choose two forms of $R(t)$ series for every case considered: (a) fixed $R(t)$ in the observational window, where $R(t)$ is a constant in any window but varies from window to window, i.e., $R(t) = R_T/T$, and (b) $R(t)$ being chosen randomly in the observational window from a uniform distribution, e.g., $(R_T/T) [0, 2]$. In both (a) and (b) the total driving R_T within each window is the same.

Equation (1) indicates that the external driving contributes to the flux fluctuation through the ratio α , implying that for external driving with different R_T distributions but the same ratio, the dependence of the flux fluctuation on the average flux should follow the same curve. Figure 2 shows simulation results for different R_T distributions but the same ratio, together with the corresponding analytical results. The simulations are performed on a scale-free network with degree distribution $P(k) \sim k^{-2.436}$, $N = 1000$ nodes, and mean degree $\langle k \rangle = 4$, which is generated by the preferential-attachment rule [11]. The routing protocol is based on the shortest path. The total observational time is 10^6 time steps. Figure 2(a) shows the results for the case of constant $R(t)$ in an observational time

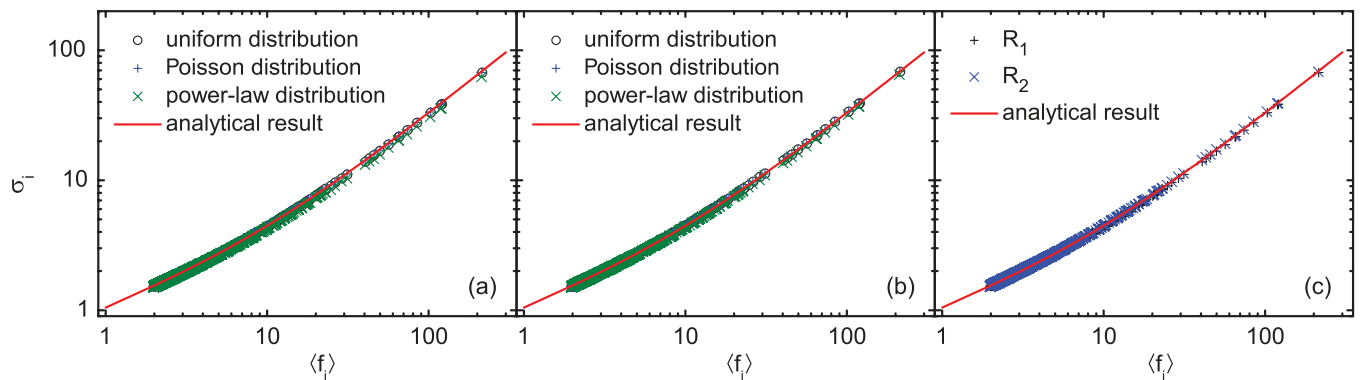


FIG. 2. (Color online) For a Barabási-Albert (BA) scale-free network with $N = 1000$ nodes and mean degree $\langle k \rangle = 4$, under the shortest-path routing protocol, nodal flux fluctuation σ_i versus the average flux $\langle f_i \rangle$ for various distributions of $R(t)$ related to external driving: (a) $R(t)$ is constant within each observational window, (b) $R(t)$ varies with time but has the same value of R_T as in (a), and (c) overlay of the two cases under uniform distribution of R_T , where R_1 is represented by circles in panel (a), and R_2 is represented by circles in panel (b). The scattered data points are simulation results from all nodes, where each point represents one node, and the solid curves are from the theoretical prediction (1). Other parameters are $T = 100$, $\langle R_T \rangle = 10T$, and $(\sigma_{R_T})^2 / \langle R_T \rangle^2 = 0.1$.

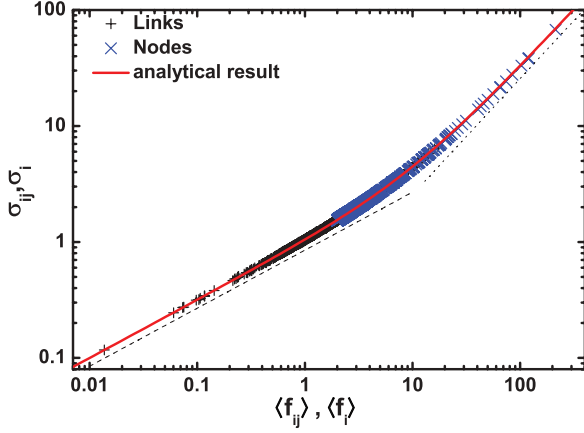


FIG. 3. (Color online) Flux fluctuation σ_{ij} (σ_i) as a function of the average flux $\langle f_{ij} \rangle$ ($\langle f_i \rangle$) for all the links (nodes) in the network. The parameters are the same as in Fig. 2(a). The solid curves are from theory [Eq. (1)]. The dashed line ($\sigma_{ij} \sim \sqrt{\langle f_{ij} \rangle}$) and the dotted line ($\sigma_{ij} \sim \langle f_{ij} \rangle$) are guides for the eye.

window and Fig. 2(b) corresponds to the case where $R(t)$ varies according to a uniform distribution in the observational window while having the same R_T distribution as in Fig. 2(a). It can be seen that, insofar as the ratio α is the same, the data points all fall on the same theoretical curve. Figure 2(c) shows, for the uniform distribution of R_T , the results from cases (a) and (b), which completely overlap with each other, corroborating that only the external driving R_T matters, while the details of the flow dynamics within the observational time window have no effect on Eq. (1). This gives strong support for the universality of Eq. (1). All these suggest that the dynamical details within the observational window have little effect on the window-to-window fluctuation behaviors.

We have also checked the fluctuation behavior of the flux through links [6], where for a link (i, j) , flows in both directions are considered and denoted by f_{ij} . In Fig. 3 we plot the flux fluctuation σ_{ij} as a function of the average flux $\langle f_{ij} \rangle$ for the links. The flux fluctuation versus the average flux of the nodes ($\sigma_i, \langle f_i \rangle$) for the same network is also plotted for comparison. The parameters are the same as in Fig. 2(a). We see that data from links and from nodes both fall on the same theoretical curve (1) with the same parameter $\alpha = 0.1$, implying that there is no difference between fluctuation phenomena observed with respect to links and nodes. One difference, is that the flux on links is typically smaller than the flux on nodes, so the link-based and node-based fluctuation-flux relations fall on different regions of the plot.

We now demonstrate that Eq. (1) holds regardless of the network topology and traffic routing protocol, despite the known fact that network structure and routing strategy can affect the traffic-flow dynamics in a significant manner [6,9,12–24]. We consider four types of well-studied network topologies: scale-free [11], random [25], small-world [26], and assortatively mixed scale-free networks [27]. The results for scale-free, random, and small-world network topologies with $R(t)$ constant and time-varying cases within the observational window are shown in Figs. 4(a) and 4(b), respectively. Results from the assortatively mixed networks are plotted in Fig. 4(c). Using the Pearson correlation coefficient r to measure the

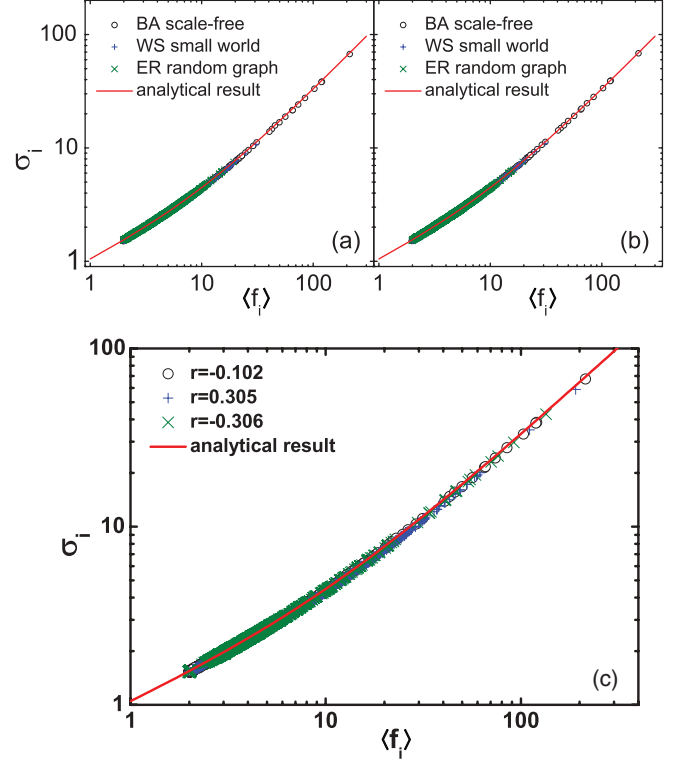


FIG. 4. (Color online) Nodal flux fluctuation σ_i versus the average flux $\langle f_i \rangle$ for complex networks of different topologies. The solid curves are from theory [Eq. (1)]. (a) $R(t)$ is constant within one observational window but varies from window to window and (b) $R(t)$ varies in every observational window. In both panels, results from BA scale-free networks with $P(k) \sim k^{-2.436}$ and $\langle k \rangle = 4$, random networks with $\langle k \rangle = 6.5$, and small-world networks with $\langle k \rangle = 4$ and rewiring probability $p = 0.3$ are shown. (c) Results from the assortatively mixed scale-free networks with $P(k) \sim k^{-2.436}$, $\langle k \rangle = 4$, and different Pearson correlation coefficient r . Other parameters are the same as in Fig. 2(a). In all cases, Eq. (1) holds.

degree correlation and a rewiring process to adjust the degree-correlation coefficient [27], we compare three scale-free networks with the same degrees for assortative cases with $r = 0.102$ and 0.305 and the disassortative network with $r = -0.306$. We see that, for all cases considered, the behaviors of flux fluctuation versus the average flux collapse into a single curve as predicted by Eq. (1), indicating that the relation holds universally with respect to different network topologies. We have also tested two different traffic routing protocols: shortest-path and efficient routing protocols [10]. As shown in Fig. 5, computations reveal that Eq. (1) holds for traffic flows on complex networks, regardless of the routing protocol used.

We now turn to the observational window issue [2,3,5]. We carry out simulations by setting $R(t)$ as a rectangular wave of period 200 and duty cycle 0.5:

$$R(t) = \begin{cases} 10, & t \in [1, 100], [201, 300], [401, 500], \dots \\ 0, & t \in [101, 200], [301, 400], [501, 600], \dots \end{cases} \quad (6)$$

The observation starts from $t = 1$ and we consider two window lengths: $T = 100$ and 200 . For the case of $T = 100$, $R_T = 1000, 0, 1000, 0, \dots$, we get $\alpha = (\sigma_{R_T})^2 / \langle R_T \rangle^2 = 1$, while for the case of $T = 200$, $R_T = 1000$, which is a constant in time;

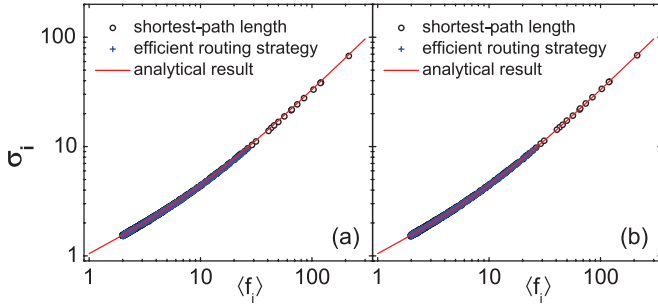


FIG. 5. (Color online) Nodal flux fluctuation σ_{f_i} as a function of $\langle f_i \rangle$ with different routing strategies. The solid curves are from theory [Eq. (1)]. (a) $R(t)$ is constant within one observational window but varies from window to window and (b) $R(t)$ varies in every observational window. Other parameters are the same as Fig. 2(a).

thus $(\sigma_{R_T})^2 = 0$ and we get $\alpha = 0$. Then, from Eq. (1) we have $\sigma_i = \sqrt{\langle f_i \rangle + \langle f_i \rangle^2}$ for $T = 100$ and $\sigma_i = \sqrt{\langle f_i \rangle}$ for $T = 200$. The simulations with $R(t)$ given by Eq. (6) are performed on a BA scale-free network with $N = 1000$, $\langle k \rangle = 4$, and the other parameters are the same as those in Fig. 2(a). The data of $(\sigma_i, \langle f_i \rangle)$ are plotted in Fig. 6, which coincide well with the analytical results. We see that, although α can be sensitive to the observational time window, the law governing the flux fluctuation and the average flux in Eq. (1) apparently holds.

All examples illustrated so far share one feature: Nodes (or links) in the network possess the same value of the ratio α , despite that the flow flux $\langle f \rangle \sim \langle R_T \rangle$ can have a wide distribution with respect to nodes (or links). As a result, the behaviors of fluctuation versus average flux for different network topologies and traffic routing protocols can all be collapsed into a single curve as given by Eq. (1). However, when there is a heterogeneous distribution of the values of α on nodes in the network, there can be distinct segments in the plot of fluctuation versus the average flux and we anticipate this situation to arise in real-world network systems, as we will demonstrate below.

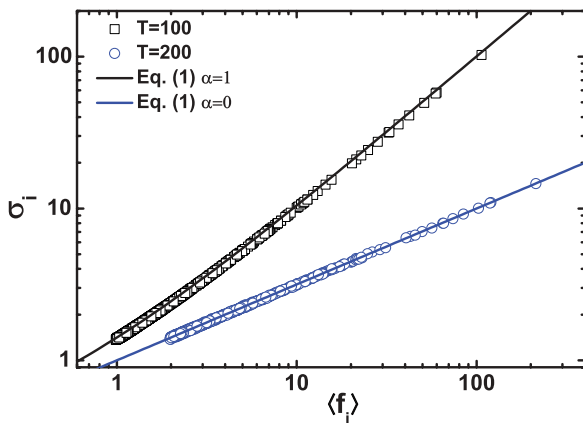


FIG. 6. (Color online) Nodal flux fluctuation σ_i as a function of $\langle f_i \rangle$ observed under observational time window $T = 100$ and 200 with external driving as a rectangular wave [see Eq. (6)]. The simulation is performed on a BA scale-free network with $N = 1000$ and $\langle k \rangle = 4$. The solid curves are from theory [Eq. (1)].

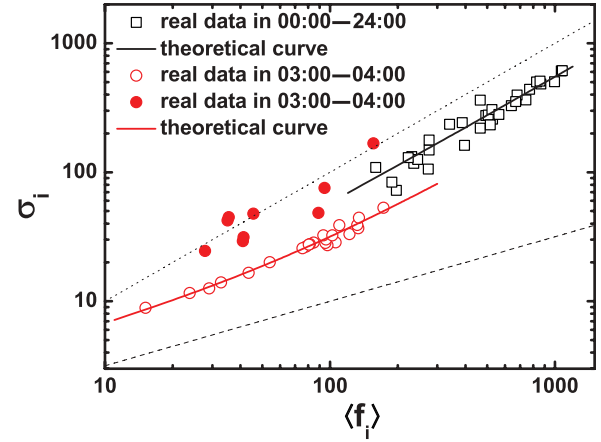


FIG. 7. (Color online) For real-world traffic data over a two-year period collected from a major city in China, flux fluctuation σ_i versus the average flux $\langle f_i \rangle$, where squares correspond to data in a whole day (00:00–24:00) and circles correspond to the data in the hourly period 03:00–04:00. The curves underlying the squares and the circles are from Eq. (1) with $\alpha^2 = 0.2989$ and 0.0604 , respectively. The dashed line ($\sigma_i \sim \sqrt{\langle f_i \rangle}$) and the dotted line ($\sigma_i \sim \langle f_i \rangle$) are guides for the eye.

IV. REAL-WORLD EXAMPLE

The real-world system we study is vehicular flow passing through 32 intersections in Lanzhou, the capital city of Gansu province in western China. The original data were collected every 15 min over 2 yr at various intersections. Each data point is the total number of vehicles that pass through the intersections over the observational window ($T = 15$ min). Since in general flux time series of traffic in social or technological systems are driven by human activities [14], the vehicular traffic flow is periodic with the period of 24 h. For each intersection i , the available data $f_i(t)$ has about 70 000 points, from which the mean $\langle f_i \rangle$ and the standard deviation σ_i can be calculated. The results for all intersections are plotted in Fig. 7 as squares, where the underlying curve is Eq. (1) for $\alpha^2 = 0.2989$. We see that the data agree well with the theory. In addition, there is a strong signature of a power-law relation as $\sigma_i \sim \langle f_i \rangle$. The reason is that the average flux $\langle f_i \rangle$ is large.

In order to reveal the fluctuation behavior for small average flux values, we divide the data set from each intersection into 24 hourly intervals. The minimum of the traffic-flow flux occurs between 3 and 4 a.m. We then take all the data points (about 3000 for each intersection) in this period and calculate the fluctuation and average for each intersection i . The results are plotted in Fig. 7 as circles, where the underlying curve is again Eq. (1) but for $\alpha^2 = 0.0604$. We observe that Eq. (1) characterizes the real data well for both relatively large and small α values. A crossover from the behavior $\sigma_i \sim \sqrt{\langle f_i \rangle}$ to $\langle f_i \rangle$ occurs about $\langle f_i \rangle = 100$. Note that there are a few outliers (solid circles). From Eq. (1), we can express the ratio α as

$$\alpha = \frac{\sqrt{\sigma_i^2 - \langle f_i \rangle}}{\langle f_i \rangle}. \quad (7)$$

We see that the value of the ratios for the outliers are indeed quite different from the values associated with the curves. For the outliers, the corresponding external driving (human

activity) during this time period has larger fluctuations σ_{R_T} than those in other “normal” intersections.

V. CONCLUSION

By considering a general setting of complex networked systems, we are able to obtain the law governing the flux fluctuation and the average flux in a straightforward manner, suggesting universal applicability of the law to complex dynamical systems. Further support for the universality is gained by extensive computations with respect to different behaviors of the external driving, different network topologies, and different traffic routing protocols. Depending on the property of the external driving, the flux-fluctuation law exhibits a crossover between power-law scaling behaviors of distinct exponents, which has been observed in a real-world vehicular traffic network. Conversely, by measuring the flux

fluctuation with respect to the mean flux, the values of the key parameter $\sigma_{R_T}/\langle R_T \rangle$ for different nodes in the network can be obtained, allowing abnormal nodes with relatively large or small driving fluctuations to be detected. This can be useful for monitoring the health of the system and controlling the system for improved performance. Fluctuation phenomena play an important role in the dynamics of complex systems. Uncovering universal phenomena is of fundamental interest. The universal flux-fluctuation law that this work aims to establish is one such example.

ACKNOWLEDGMENTS

We thank Jiaqi Dong for helpful discussions. This work was partially supported by the NSF of China under Grants No. 11275003, No. 11135001, and No. 10905026. Y.-C.L. was supported by AFOSR under Grant No. FA9550-10-1-0083.

-
- [1] M. A. de Menezes and A.-L. Barabási, *Phys. Rev. Lett.* **92**, 028701 (2004).
 - [2] J. Duch and A. Arenas, *Phys. Rev. Lett.* **96**, 218702 (2006).
 - [3] S. Meloni, J. Gómez-Gardeñes, V. Latora, and Y. Moreno, *Phys. Rev. Lett.* **100**, 208701 (2008).
 - [4] Z. Eisler and J. Kertész, *Phys. Rev. E* **71**, 057104 (2005).
 - [5] S. Yoon, S.-H. Yook, and Y. Kim, *Phys. Rev. E* **76**, 056104 (2007).
 - [6] B. Kujawski, B. Tadić, and G. J. Rodgers, *New J. Phys.* **9**, 154 (2007).
 - [7] S. He, S. Li, and H. R. Ma, *Eur. Phys. J. B* **76**, 31 (2010).
 - [8] V. Kishore, M. S. Santhanam, and R. E. Amritkar, *Phys. Rev. Lett.* **106**, 188701 (2011).
 - [9] P. Echenique, J. Gómez-Gardeñes, and Y. Moreno, *Phys. Rev. E* **70**, 056105 (2004); *Europhys. Lett.* **71**, 325 (2005).
 - [10] G. Yan, T. Zhou, B. Hu, Z.-Q. Fu, and B.-H. Wang, *Phys. Rev. E* **73**, 046108 (2006).
 - [11] A.-L. Barabási and R. Albert, *Science* **286**, 509 (1999).
 - [12] A. Arenas, A. Díaz-Guilera, and R. Guimerà, *Phys. Rev. Lett.* **86**, 3196 (2001).
 - [13] J.-T. Sun, S.-J. Wang, Z.-G. Huang, and Y.-H. Wang, *Physica A* **388**, 3244 (2009).
 - [14] Z. Zhou, Z.-G. Huang, L. Yang, D.-S. Xue, and Y.-H. Wang, *J. Stat. Mech.* (2010) P08001.
 - [15] K.-I. Goh, B. Kahng, and D. Kim, *Phys. Rev. Lett.* **87**, 278701 (2001).
 - [16] R. Guimerà, A. Díaz-Guilera, F. Vega-Redondo, A. Cabrales, and A. Arenas, *Phys. Rev. Lett.* **89**, 248701 (2002).
 - [17] P. Holme and B. J. Kim, *Phys. Rev. E* **65**, 066109 (2002).
 - [18] W.-X. Wang, B.-H. Wang, B. Hu, G. Yan, and Q. Ou, *Phys. Rev. Lett.* **94**, 188702 (2005).
 - [19] B. Danila, Y. Yu, J. A. Marsh, and K. E. Bassler, *Phys. Rev. E* **74**, 046106 (2006).
 - [20] W. X. Wang, B. H. Wang, C. Y. Yin, Y. B. Xie, and T. Zhou, *Phys. Rev. E* **73**, 026111 (2006).
 - [21] X. Ling, M.-B. Hu, R. Jiang, R. Wang, X.-B. Cao, and Q.-S. Wu, *Phys. Rev. E* **80**, 066110 (2009).
 - [22] O. Narayan and I. Sanjeev, *Phys. Rev. E* **82**, 036102 (2010).
 - [23] S. Meloni and J. Gómez-Gardeñes, *Phys. Rev. E* **82**, 056105 (2010).
 - [24] J. J. Ramasco, M. S. de La Lama, E. López, and S. Boettcher, *Phys. Rev. E* **82**, 036119 (2010).
 - [25] P. Erdős and A. Rényi, *Publ. Math.* **5**, 17 (1960).
 - [26] D.-J. Watts and S. H. Strogatz, *Nature (London)* **393**, 440 (1998).
 - [27] M. E. J. Newman, *Phys. Rev. Lett.* **89**, 208701 (2002).